Experimental Parameter Extraction in the Single-Diode Photovoltaic Model via a Reduced-Space Search

Alejandro Angulo Cárdenas, *Member, IEEE*, Miguel Carrasco, Fernando Mancilla-David, *Member, IEEE*, Alexandre Street, *Member, IEEE*, and Roberto Cárdenas, *Senior Member, IEEE*

***Abstract*—The behavior of a photovoltaic (PV) module may be captured via its current–voltage (I–V) characteristic. The single-diode model is able to adequately fit this characteristic while featuring limited parameterization difficulty, and is thus widely adopted to represent the performance of a PV module. However, the identification of the model's parameters is a complex task due to the nonconvex nature of the underlying optimization problem. In this paper, an efficient method for the parameter extraction of the single-diode PV model from experimental I–V curves is developed. This method features two advantages with respect to the existing procedures. On the one hand, it is able to find high-quality solutions at a reduced computational complexity. On the other hand, it does not rely on any preliminary data selection and it can thus be fully automated without user intervention. Numerical results obtained for case studies common in the literature and a large-scale repository show its performance. A computer program implementing the proposed methodology is available upon request via an e-mail to all interested researchers.**

***Index Terms*—Optimization methods, parameter estimation, photovoltaic (PV) cells.**

I. Introduction

PHOTOVOLTAIC (PV) power generation is increasingly becoming a commodity, as the technology costs have steadily declined and pathways to further cost reductions are being pursued. By the end of the decade, both distributed and large-scale PV generation are expected to be cost competitive with retail electricity prices without subsidies in a significant portion of the world [1]. In a PV system, the conversion of light into electricity takes place at the PV cells, which can be connected in series and in parallel to form PV modules. The behavior of a PV module may be captured via a static relationship that describes its current–voltage (I–V) characteristic. Single-diode- and two-diode-based models have been proposed to reproduce this characteristic [2]. The single-diode model is able to adequately fit the I–V curve while featuring limited parameterization difficulty, and is thus widely adopted to represent the performance of a PV module [3], [4].

The parameters of the single-diode model can be extracted via two different approaches. On the one hand, manufacturer's datasheets specify a set of typical operating points and temperature sensitivities, which makes a consistent parameter identification possible. Many methodologies have been proposed to make the use of the available data—see for example [5]–[8] and references therein. The outcome of these methods are reference parameters to be used in single-diode models that are able to reproduce the behavior of a PV module under varying atmospheric conditions.

On the other hand, model parameters can be extracted from an experimental I–V curve utilizing nonlinear regressions, which, in general, involve the solution of nonconvex and NP-hard optimization problems. In the cases where a "certified" high-quality solution is needed, global optimization techniques ought to be used. However, such techniques are scarce, computationally expensive, and cannot be considered as a mature technology. If only feasible solutions are sought, local interior point solvers can be used, but convergence to a global optimum is not guaranteed and the final solution is highly dependent on the starting point. Because of this, the problem of parameter extraction from experimental I–V curves has been approached through a myriad of heuristic-based algorithms [9]–[15]. Although some of them are effective in finding high-quality solutions (though not certified), the computational cost of these methods is significant.

Recently, two heuristics that follow a more deterministic approach have appeared in the literature [16], [17]. Lim *et al.* [16] *assume* the I–V curve to be the output of a linear system, and the model parameters are extracted by identifying the parameters of a linear differential equation. In [17], the idea of a reduced-space search was first proposed, but relies on the *preliminary manipulation* of the I–V curve by making the use of additional information, such as the short circuit current (I_{sc}), open circuit

Manuscript received May 12, 2016; revised August 4, 2016; accepted August 24, 2016. Date of publication October 6, 2016; date of current version January 10, 2017. The work of A. Angulo Cárdenas and R. Cárdenas was supported by the Chilean Government under Fondecyt Project #3160209. The work of F. Mancilla-David and A. Street was supported in part by the Brazilian Government under CNPq Grant #405644/2015–9. The work of F. Mancilla-David was also supported by the Fulbright Foundation.

A. Angulo Cárdenas and R. Cárdenas are with the Department of Electrical Engineering, University of Chile, Santiago 1058, Chile (e-mail: alejandro.a.angulo@gmail.com; rcd@ieee.org).

M. Carrasco and F. Mancilla-David are with the Department of Electrical Engineering, University of Colorado Denver, Denver, CO 80204 USA (e-mail: miguel.carrasco.lopez@gmail.com; Fernando.Mancilla-David@ucdenver.edu).

A. Street is with the Department of Electrical Engineering, Pontifical Catholic University of Rio de Janeiro, Rio de Janeiro 38097, Brazil (e-mail: street@ele.puc-rio.br).

Color versions of one or more of the figures in this paper are available online at http://ieeexplore.ieee.org.

Digital Object Identifier 10.1109/TIE.2016.2615590

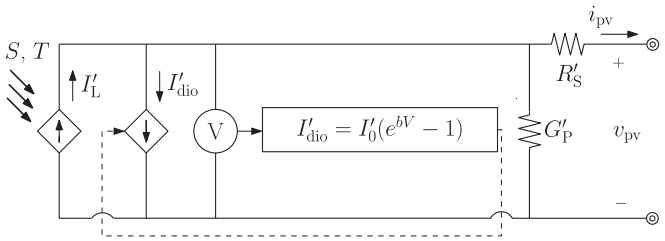

Fig. 1. Equivalent circuit of a PV array.

voltage ($V_{\rm oc}$), and maximum power point (MPP) ($V_{\rm mpp}, I_{\rm mpp}$). The quality of the solution achieved by this method depends on the accuracy of this data, which in many cases needs to be roughly estimated. The aforementioned methods provide parameter values valid only for the atmospheric conditions at which the corresponding I–V curve was measured. If a set of curves at different atmospheric conditions is available, these methods may be used as a mean to study parameter dependencies, and therefore set the basis to improve the modeling of PV modules [18], [19]. Furthermore, if their computational complexity is reduced, they may be employed in the field for online monitoring and diagnostics, and for automated outdoor module testing [16].

In this paper, an efficient heuristic based on a reduced-space search for the parameter extraction from experimental I–V curves is proposed. This method features two advantages with respect to the existing procedures. On the one hand, it is able to find high-quality solutions at a reduced computational complexity. On the other hand, the work presented here does not rely on any preliminary data selection, as it is done in [17], and it can thus be fully automated without user intervention. The key aspect of computing a reduced space for solution search is achieved by a number of educated assumptions starting from the original nonconvex mathematical programming problem.

The paper is organized as follows. Section II reviews the single-diode model, which is the basis for this work. In Section III, the problem of parameter extraction from experimental curves is explained. In Section IV, an efficient method to solve this problem via a reduced-space search space is formulated. Numerical results are shown in Section V for case studies common in the literature and a large-scale repository. In Section VI, the potential of the methodology is demonstrated through the evaluation of the parameter dependencies for a PV module belonging to the heterojunction with intrinsic thin-layer technology. Finally, the conclusions are given in Section VII.

II. Single-Diode PV Model

The behavior of a single PV cell and its generalization to a number of cells in series may be captured by the single-diode model presented in [3], whereas its application to a PV array of arbitrary configuration was accomplished in [20]. A single circuital representation can therefore be used to reproduce the behavior of an arbitrary number of cells connected in series N_S and in parallel N_P, as shown in Fig. 1. The model takes the form of

$$i_{\rm PV} = f(i_{\rm PV}, v_{\rm PV}) = I'_L - I'_0(e^{b(v_{\rm PV} + i_{\rm PV} R'_S)} - 1) - G'_P\,(v_{\rm PV} + i_{\rm PV} R'_S) \qquad (1)$$

where b is the reciprocal of the modified ideality factor, computed as

$$b = \frac{q}{N_S n k T} \qquad (2)$$

in terms of the electron's electric charge $q = 1.602 \times 10^{-19}$ C, the Boltzmann constant $k = 1.3806503 \times 10^{-23}$ J/K, and the ideality factor of the diode n. The various "prime" parameters are related to their cell-specific counterparts according to

$$R'_S := \frac{N_S}{N_P} R_S,\ I'_L := N_P I_L,\ I'_0 := N_P I_0,\ G'_P := \frac{N_P}{N_S} G_P \qquad (3)$$

where I_L is the photoelectric current generated when the cell is exposed to sunlight; I_0 is the diode saturation current or cell reverse saturation current; and R_S and G_P represent the cell series resistance and shunt admittance, respectively [3], [21].

The curve represented by (1) is a good fit to the experimental characteristic of a PV module when its five parameters are determined for the irradiance (S) and temperature (T) conditions at which the curve was measured [18]. In order to reproduce I–V characteristics at varying conditions, additional sets of equations have been proposed to capture the corresponding dependencies [22]–[24].

III. Parameter Extraction From Measured I–V Curves

The problem at hand consists in finding the value of the five parameters in (1) which make such equation best fit an experimental I–V curve. The vector

$$\boldsymbol{x} = [b\ \ R_S\ \ I_L\ \ I_0\ \ G_P]^T$$

collects the parameters. It is noteworthy that these parameters may be replaced by their "primed" counterparts through (3) to account for an arbitrary PV array configuration. However, since it does not impact the mathematical considerations explained in this paper, "primes" will be omitted for the sake of notational simplicity.

Hereinafter, vectors are assumed to be a column vector unless otherwise noted. Index notation will be used to specify the elements of a vector, that is, the kth element of the vector $\boldsymbol{x}$ will be x_k. Transpose operator of vector $\boldsymbol{x}$ will be denoted as $\boldsymbol{x}^T$. Inner product between vectors $\boldsymbol{x}$ and $\boldsymbol{y}$ will be expressed as $\boldsymbol{x}^T\boldsymbol{y}$.

The mathematical programming problem for the estimation of $\boldsymbol{x}$ is presented in (P0). It corresponds to a standard error-in-variables formulation [25], that seeks to minimize the weighted sum of squared errors between the measured currents and voltages (I_k, V_k) and those predicted by the model $(\tilde{I}_k, \tilde{V}_k)$, subject to the model equation

$$\text{(P0)}\quad \min_{\boldsymbol{x}, \tilde{I}_k, \tilde{V}_k} \sum_{k\in\mathcal{M}} \left(\frac{\tilde{I}_k - I_k}{\sigma_I}\right)^2 + \left(\frac{\tilde{V}_k - V_k}{\sigma_V}\right)^2$$

s.t.

$$f(\boldsymbol{x}, \tilde{I}_k, \tilde{V}_k) - \tilde{I}_k = 0 \qquad \forall\, k \in \mathcal{M},$$
$$\boldsymbol{x} \in \mathbb{R}^5_+$$

In (P0), $\mathcal{M} = \{1, \ldots, M\}$ represents the set of M measurements and (σ_I, σ_V) are the corresponding standard deviations.

Also, the physical interpretation of the parameters restrict all entries of $\boldsymbol{x}$ to be nonnegative.

A common approach to make this problem more tractable is to assume that one of the variables has a very small variance. Typically, this variable is the PV voltage. If $\sigma_V \to 0$, then the second term in the objective must be zero—which implies $\tilde{V}_k = V_k$—and problem (P0) can be rewritten as follows:

$$\begin{aligned}(\text{P1}) \quad & \min_{\boldsymbol{x},\tilde{\boldsymbol{I}}} (\tilde{\boldsymbol{I}}-\boldsymbol{I})^T(\tilde{\boldsymbol{I}}-\boldsymbol{I}) \\ \text{s.t.} \quad & \\ & f(\boldsymbol{x},\tilde{I}_k,V_k)-\tilde{I}_k = 0 \qquad \forall\, k \in \mathcal{M} \\ & \boldsymbol{x} \in \mathbb{R}^5_+\end{aligned}$$

where vector notation is introduced for the sake of simplicity and, without loss of generality, σ_{I} is assumed to be one. The transcendental nature of (1) does not allow for an explicit computation of $\tilde{I}_k$ in the equality constraint of (P1). One approach to overcome this issue is through utilizing the Lambert W function [26], which allows us to solve for $\tilde{I}_k$:

$$\tilde{I}_k = f^W(x,V_k) = \frac{I_L + I_0 - G_{\mathrm{p}}V_k}{R_{\mathrm{s}}G_{\mathrm{p}}+1} - \frac{1}{bR_{\mathrm{s}}} W\left[\frac{bR_{\mathrm{s}}I_0}{R_{\mathrm{s}}G_{\mathrm{p}}+1} e^{b\frac{R_{\mathrm{s}}(I_L+I_0)+V_k}{R_{\mathrm{s}}G_{\mathrm{p}}+1}}\right]$$

and problem (P1) can be reformulated as a nonnegative least squares problem as follows:

$$(\text{P2}) \qquad \min_{\boldsymbol{x}\in\mathbb{R}^5_+} \sum_{k\in\mathcal{M}} \left(f^W(\boldsymbol{x},V_k)-I_k\right)^2.$$

The complexity of the parameter extraction task lies in the nonlinear nonconvex nature of the regression model (P2), which leads to the existence of multiple local optima. Furthermore, it is not separable and it has to be solved in the search space defined by $\boldsymbol{x}$, which is the five-dimensional (5-D) nonnegative orthant. If an ε-optimal solution is needed, then the global optimization techniques ought be used. In most of the practical cases the certification of the solution quality can be relaxed, which allows us to approach the solution of the problem via heuristic-based methods. Many of these methods have been proposed in the literature, but their tradeoff between the solution quality and computational cost is low [9]–[15]. Deterministic solving methods (e.g., trust-region or Levenberg–Marquardt methods) may in this case be casted as heuristic approaches, because they are able to find local optima only depending on the selection of the initial guess $\boldsymbol{x}_0$ [17]. Furthermore, a local optimizer may not even have a proper physical correspondence [24]. An approach to find high-quality solutions using this type of approach is proposed in [27] and [17], where reduced forms are used to project the 5-D search space into a 2-D one. In this spirit, an alternative procedure is proposed in the next section.

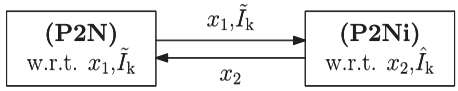

Fig. 2. Couplings between outer- and inner-nested problems.

IV. Efficient Parameter Extraction via a Reduced-Space Search Approximation

The method proposed herein seeks to decrease the complexity of the parameter extraction by performing an educated approximation of the problem (P2) and a subsequent dimensionality reduction of its search space. This allows finding high-quality solutions which may also be used as initial guesses for the original problem. Toward this end, problem (P2) is reformulated through an extended form as follows:

$$\begin{aligned}(\text{P2E}) \quad & \min_{\boldsymbol{x},\tilde{\boldsymbol{I}},\hat{\boldsymbol{I}}} (\tilde{\boldsymbol{I}}-\boldsymbol{I})^T(\tilde{\boldsymbol{I}}-\boldsymbol{I}) + (\hat{\boldsymbol{I}}-\tilde{\boldsymbol{I}})^T(\hat{\boldsymbol{I}}-\tilde{\boldsymbol{I}}) \\ \text{s.t.} \quad & \\ & f^W(x,V_k)-\tilde{I}_k = 0 \qquad \forall\, k \in \mathcal{M} \\ & f(x,\tilde{I}_k,V_k)-\hat{I}_k = 0 \qquad \forall\, k \in \mathcal{M} \\ & \boldsymbol{x} \in \mathbb{R}^5_+\end{aligned}$$

where $\hat{I}_k$ is an auxiliary variable that enables the extended formulation (P2E). It takes the same value as $\tilde{I}_k$ as implied by the second equality constraint in (P2E). The minimizer of (P2E) is thus the same as that of (P2). The reformulation enables a generalized Benders-like decomposition of the problem [28] with two reduced decision vectors:

$$\boldsymbol{x}_1 = [b \;\; R_S]^T$$
$$\boldsymbol{x}_2 = [I_L \;\; I_0 \;\; G_P]^T$$

via the following nested form:

$$\begin{aligned}(\text{P2N}) \quad & \min_{\boldsymbol{x}_1,\tilde{\boldsymbol{I}}} (\tilde{\boldsymbol{I}}-\boldsymbol{I})^T(\tilde{\boldsymbol{I}}-\boldsymbol{I}) + \varphi(\boldsymbol{x}_1,\tilde{\boldsymbol{I}}) \\ \text{s.t.} \quad & \\ & f^{\mathrm{W}}(\boldsymbol{x}_1,\boldsymbol{x}_2,V_k)-\tilde{I}_k = 0 \qquad \forall\, k \in \mathcal{M} \\ & \boldsymbol{x}_1 \in \mathbb{R}^2_+ \\ & (\boldsymbol{x}_1,\tilde{\boldsymbol{I}}) \in F_\varphi\end{aligned}$$

where

$$\begin{aligned}(\text{P2Ni}) \quad & \varphi(\boldsymbol{x}_1,\tilde{\boldsymbol{I}}) = \min_{\boldsymbol{x}_2,\hat{\boldsymbol{I}}} (\hat{\boldsymbol{I}}-\tilde{\boldsymbol{I}})^T(\hat{\boldsymbol{I}}-\tilde{\boldsymbol{I}}) \\ \text{s.t.} \quad & \\ & f(\boldsymbol{x}_1,\boldsymbol{x}_2,\tilde{I}_k,V_k)-\hat{I}_k = 0 \qquad \forall\, k \in \mathcal{M} \\ & \boldsymbol{x}_2 \in \mathbb{R}^3_+\end{aligned}$$

and F_φ is the set of pairs $(\boldsymbol{x}_1,\tilde{\boldsymbol{I}})$ for which the problem (P2Ni) has a feasible solution. Nonconvexities and couplings between the outer problem (P2N) and the inner problem (P2Ni)—as depicted in Fig. 2—prevent finding a solution for the former in a simple way (e.g., by using standard nonlinear least squares solvers).

To overcome these issues, problem (P2Ni) may be approximated by assuming $\tilde{\boldsymbol{I}} \simeq \boldsymbol{I}$, which is the relaxed solution of the problem (P2E) when all constraints are relaxed:

$$\begin{aligned}(\text{P2Ni}')\quad & \varphi(\boldsymbol{x}_1) = \min_{\boldsymbol{x}_2, \hat{\boldsymbol{I}}} (\hat{\boldsymbol{I}} - \boldsymbol{I})^T (\hat{\boldsymbol{I}} - \boldsymbol{I}) \\ \text{s.t.}\quad & \\ & f(\boldsymbol{x}_1, \boldsymbol{x}_2, I_k, V_k) - \hat{I}_k = 0 \qquad \forall\, k \in \mathcal{M} \\ & \boldsymbol{x}_2 \in \mathbb{R}^3_+.\end{aligned}$$

Given $\boldsymbol{x}_1$, constraints in (P2Ni') are linear, and therefore (P2Ni') may be casted as an ordinary nonnegative least squares problem [29]. This problem may be solved by an ad hoc numerical solver, but it is well known that (P2Ni') is ill-conditioned, so such solver is likely to be unstable. To overcome this issue, an analytical solution utilizing some educated approximations is proposed. If the nonnegative constraints of (P2Ni') are relaxed, the value of $\boldsymbol{x}_2$ can be found through a closed-form expression by solving the corresponding normal equation:

$$\underbrace{\begin{bmatrix} \mathbf{1}^T \boldsymbol{I} \\ \boldsymbol{E}^T \boldsymbol{I} \\ \boldsymbol{D}^T \boldsymbol{I} \end{bmatrix}}_{\mathrm{B}(\boldsymbol{x}_1)} = \underbrace{\begin{bmatrix} \mathbf{1}^T \mathbf{1} & \mathbf{1}^T \boldsymbol{E} & \mathbf{1}^T \boldsymbol{D} \\ \boldsymbol{E}^T \mathbf{1} & \boldsymbol{E}^T \boldsymbol{E} & \boldsymbol{E}^T \boldsymbol{D} \\ \boldsymbol{D}^T \mathbf{1} & \boldsymbol{D}^T \boldsymbol{E} & \boldsymbol{D}^T \boldsymbol{D} \end{bmatrix}}_{\mathrm{A}(\boldsymbol{x}_1)} \underbrace{\begin{bmatrix} I_L \\ I_0 \\ G_P \end{bmatrix}}_{\boldsymbol{x}_2} \tag{4}$$

where $\mathbf{1}$ is the M-dimensional vector of unit entries and $\boldsymbol{D}$ and $\boldsymbol{E}$ are the vectors of size M, whose elements may be computed as

$$\begin{aligned} D_k &= D_k(\boldsymbol{x}_1) = 1 - e^{b(V_k + R_S I_k)} \\ E_k &= E_k(\boldsymbol{x}_1) = -V_k - R_S I_k \qquad \forall\, k \in \mathcal{M}. \end{aligned}$$

As a consequence of the relaxation of the nonnegativity constraints, nonphysically valid solutions are possible. When this happens, the following alternative procedure in the spirit of the active set method to solve nonnegative least squares problems [30] may be leveraged. If a nonnegativity constraint is violated, then it is forced to equality by modifying (4). Specifically, in the case that G_P is negative, (4) is replaced with

$$\begin{bmatrix} \mathbf{1}^T \boldsymbol{I} \\ \boldsymbol{E}^T \boldsymbol{I} \\ G_{\mathrm{P,fixed}} \end{bmatrix} = \begin{bmatrix} \mathbf{1}^T \mathbf{1} & \mathbf{1}^T \boldsymbol{E} & \mathbf{1}^T \boldsymbol{D} \\ \boldsymbol{E}^T \mathbf{1} & \boldsymbol{E}^T \boldsymbol{E} & \boldsymbol{E}^T \boldsymbol{D} \\ 0 & 0 & 1 \end{bmatrix} \begin{bmatrix} I_L \\ I_0 \\ G_P \end{bmatrix} \tag{5}$$

where $G_{\mathrm{P,fixed}}$ may be set to an arbitrarily small positive value. Correspondingly, if I_0 is negative, (4) may be modified to

$$\begin{bmatrix} \mathbf{1}^T \boldsymbol{I} \\ I_{0,\mathrm{fixed}} \\ \boldsymbol{D}^T \boldsymbol{I} \end{bmatrix} = \begin{bmatrix} \mathbf{1}^T \mathbf{1} & \mathbf{1}^T \boldsymbol{E} & \mathbf{1}^T \boldsymbol{D} \\ 0 & 1 & 0 \\ \boldsymbol{D}^T \mathbf{1} & \boldsymbol{D}^T \boldsymbol{E} & \boldsymbol{D}^T \boldsymbol{D} \end{bmatrix} \begin{bmatrix} I_L \\ I_0 \\ G_P \end{bmatrix} \tag{6}$$

where $I_{0,\mathrm{fixed}}$ may be set to an arbitrarily small positive value. A similar approach could be followed if I_L is negative. However, this case did not arise during the extensive computational experiments carried out in this work.

Algorithm 1: Proposed Parameter Extraction Procedure.

Require: Initial guess $\boldsymbol{x}_1^{(0)}$. Control flag for refinement option.
Ensure: Identified parameters $\boldsymbol{x}^* = [\boldsymbol{x}_1^{*T} \quad \boldsymbol{x}_2^{*T}]^T$.
1: $\boldsymbol{x}_1 \leftarrow \boldsymbol{x}_1^{(0)}$
2: Update $\boldsymbol{x}_1$ by solving problem **(P3)**. Replace (4) by (5) or (6) as needed to ensure a physically valid solution.
3: Update $\boldsymbol{x}_2$ from $\boldsymbol{x}_1$ through (7).
4: **if** Refinement option is enabled **then**
5: Update $\boldsymbol{x}$ by solving the problem **(P2)** with current $\boldsymbol{x}_1$, $\boldsymbol{x}_2$ as initial values (optional).
6: **return** $\boldsymbol{x}^* \leftarrow \boldsymbol{x}$

From the above discussion it is clear that the optimal value for $\boldsymbol{x}_2$ can be determined for a given $\boldsymbol{x}_1$ as

$$\boldsymbol{x}_2 = \mathrm{C}(\boldsymbol{x}_1)\ \mathrm{B}(\boldsymbol{x}_1) \tag{7}$$

where $\mathrm{C} = \mathrm{A}^{-1}$. It is noteworthy to say that A may be ill-conditioned. However, C can be easily obtained by finding an algebraic expression for the inverse of a symmetric 3×3 matrix. Mapping (7) can now be leveraged to replace the nested optimization problem with

$$\begin{aligned}(\text{P3})\quad & \min_{\boldsymbol{x}_1, \tilde{\boldsymbol{I}}} (\tilde{\boldsymbol{I}} - \boldsymbol{I})^T (\tilde{\boldsymbol{I}} - \boldsymbol{I}) \\ \text{s.t.}\quad & \\ & f^{\mathrm{W}}(\boldsymbol{x}_1, \boldsymbol{x}_2, \tilde{I}_k, V_k) - \tilde{I}_k = 0 \qquad \forall k \in \mathcal{M} \\ & \boldsymbol{x}_2 = \mathrm{C}(\boldsymbol{x}_1)\ \mathrm{B}(\boldsymbol{x}_1) \\ & \boldsymbol{x}_1 \in \mathbb{R}^2_+.\end{aligned}$$

Note that $\varphi(\boldsymbol{x}_1, \tilde{I}_k)$ in the objective function and the constraint F_φ have been neglected to further simplify the problem. Usually, values of b are lower bounded by critical values of the diode ideality factor $n_{\max}$ as

$$b \geq \frac{q}{k} \frac{1}{n_{\max} N_S T}$$

and a tighter box constraint needs to be considered for b. In this paper, $n_{\max} = 5$ is assumed.

Through (P3), the parameter extraction problem is formulated in the reduced-space search defined by the 2-D decision vector $\boldsymbol{x}_1$. This allows for finding high-quality solutions at a reduced computational cost. However, if a higher accuracy is desired, this solution may be used as an initial point to solve the original problem (P2). As numerical results show in Section V, this second stage may be considered as an optional solution refinement, since the results obtained by solving (P3) are in general of satisfactory quality. The procedure is formalized as Algorithm 1.

V. Numerical Results

The proposed approach is validated through two sets of experiments. In the first one, two case studies commonly used in the literature are selected in order to perform a comparative evaluation against the best documented solutions. In the second one,

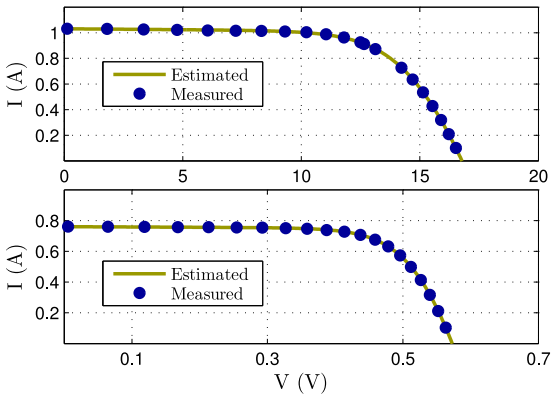

Fig. 3. Measured and estimated I–V curves for case study 1 (top) and 2 (bottom).

TABLE I
RESULTS FOR CASE STUDIES 1 AND 2

	1 (a)	1 (b)	2 (a)	2 (b)
b (1/V)	0.769094	0.769022	25.658612	25.658612
R_S (Ω)	1.238972	1.239060	0.036547	0.036547
I_L (A)	1.032345	1.032377	0.760788	0.760788
I_0 (μA)	2.515158	2.517957	3.106845E-1	3.106847E-1
G_P (S)	0.001337	0.001341	0.018907	0.018907

the performance of the proposed methodology is shown through its application to a large-scale repository of I–V curves.

A. Experiment 1: Case Studies

The two case studies considered are presented in [17] and correspond to: 1) the I–V curve of the solar module Photowatt-PWP 201, in which 36 polycrystalline silicon cells are connected in series at 1000 W/m^2 and 45° C; and 2) the I–V curve of a 57 mm diameter RTC France silicon solar cell at 1000 W/m^2 and 33° C. The measurements characterizing these curves are depicted in Fig. 3.

The proposed parameter extraction procedure was implemented in MATLAB (Release 2013a) using the function `lsqnonlin`, where box constraints on variables are included. The experiments were performed under Windows 7 (64 bits) operating system on an Intel Core i7 3.50 GHz CPU with 16 GB of memory. For the selection of initial values, b was set to its lower bound and R_S to $0.005 \times (\max\{V_k\}/\max\{I_k\})$. The Lambert function was evaluated according to [31] and [32].

Table I shows the results for case studies 1 and 2, following the proposed method (a) without and (b) with solution refinement. It is shown that the difference between the two solutions in each case study is very small. This is further demonstrated through the computation of the corresponding root-mean-square error (RMSE) values, shown in Table II, where the best-documented case in the literature was also included [17]. As it can be seen, the proposed method with refinement yields the same RMSE values as the best case. If the refinement stage is not utilized, solutions are found at a significantly reduced computational cost, while the RMSE value is only 0.015% higher for case study 1 and remains the same for case study 2. The estimated I–V curves

TABLE II
RMSE VALUES, NUMBER OF STEPS, AND NUMBER OF FUNCTION EVALUATIONS (FES) FOR CASE STUDIES 1 AND 2

Case study 1	RMSE	Steps	FEs
Best documented	2.0465E-3	19	147
1 (a)	2.0468E-3	10	33
1 (b)	2.0465E-3	27	141
Case study 2	**RMSE**	**Steps**	**FEs**
Best documented	7.7301E-4	16	138
2 (a)	7.7301E-4	7	24
2 (b)	7.7301E-4	8	36

TABLE III
ELECTRICAL PARAMETERS DEDUCED FROM THE IDENTIFIED MODEL FOR CASE STUDIES 1 AND 2

	1 (a)	1 (b)	2 (a)	2 (b)
V_{oc} (V)	16.776936	16.777001	0.572780	0.572780
I_{sc} (A)	1.030634	1.030660	0.760262	0.760262
V_{mpp} (V)	12.655356	12.655181	0.450685	0.450685
I_{mpp} (A)	0.912685	0.912652	0.689383	0.689383

which result from evaluating (1) with the obtained solutions for the two case studies are shown in Fig. 3.

Another advantage of the proposed approach is that there is no preliminary data selection, and the solution obtained is unique. On the contrary, in [17] the identification process depends on a preliminary selection of data—I_{sc}, V_{oc}, V_{mpp}, I_{mpp}—which may lead to results of different quality. After identifying five parameters of the single-diode model, it is possible to accurately compute I_{sc}, V_{oc}, V_{mpp}, and I_{mpp}, as shown in Table III. These values deviate from the estimates assumed in [17] for the identification process, which highlights the drawback of that methodology.

Finally, the proposed approach is also effective when only a limited amount of measurements is available—even if they do not span across the whole operating range. This is especially relevant considering that in some applications only measurements near the MPP can be obtained. Under these conditions existing methodologies are limited, while the proposed one is robust and allows for finding valid solutions. This is demonstrated by solving case studies 1 and 2 with only 50% of the measurements, selecting those closest to the MPP, as shown in Fig. 4. RMSE values—computed with respect to the full set of measurements—obtained when applying the proposed method without refinement are 1.05×10^{-2} and 1.57×10^{-2}, respectively.

B. Experiment Set 2: Large-Scale I–V Curve Repository

In the second set of experiments, a large-scale repository publicly available through the National Renewable Energy Laboratory is considered [19]. This repository includes a large number of I–V curves under a wide range of atmospheric conditions, representing each season in three climatically diverse locations within US territory: Cocoa, Florida (subtropical climate);

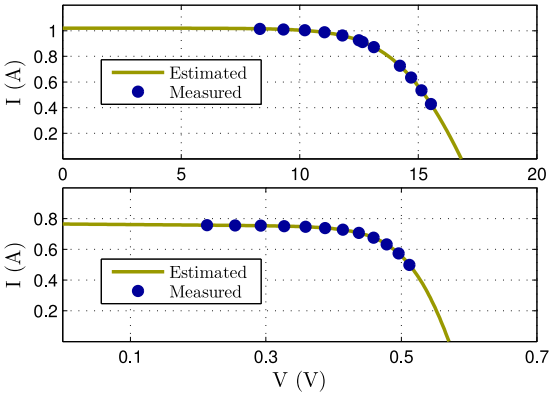

Fig. 4. Measured and estimated I–V curves for case study 1 (top) and 2 (bottom) with a reduced number of measurements.

TABLE IV
SOLUTION TIMES OBTAINED WITH MATLAB AND ANSI–C IMPLEMENTATIONS (SEC), AND THE CORRESPONDING SPEED-UP FACTORS

	MATLAB	ANSI–C	Speed-up factor
1 (a)	0.8024	0.0150	53.4
1 (b)	3.6210	0.0460	78.8
2 (a)	0.4172	0.0150	27.8
2 (b)	0.6365	0.0160	39.8

Eugene, Oregon (marine west coast climate); and Golden, Colorado (semiarid climate).

A total of 22 PV modules were tested, including eight different flat-plate PV technologies. The I–V curves were measured every five minutes for approximately one-year periods, yielding a total of 1 025 599 measurements. In order to efficiently apply the proposed methodology to this large-scale data set, the programming language ANSI–C and the libraries GSL [33] and MPFIT [34] were utilized to solve the algebraic and optimization problems, respectively. The computational advantage of this implementation is shown in Table IV, where solution times using MATLAB and ANSI–C implementations were measured when applied to the case studies of the previous section. It can be seen that the ANSI–C implementation yields speed-up factors of up to 78.8.

The proposed solution method without refinement was utilized to extract the five parameters of (1) from all the I–V curves in the large-scale repository. The resulting average RMSE and mean absolute error (MAE) values were 6.65×10^{-3} and 5.61×10^{-3}, respectively, and the average solution time was 11.2 msec. In a second step, the solution method with refinement was applied, yielding reduced average RMSE and MAE values of 3.32×10^{-3} and 2.68×10^{-3}, while the average solution time increased to 34.6 msec. Detailed performance indicators of the applied solution method without and with refinement for all PV modules included in the repository are shown in Tables V and VI, respectively. For each PV module, the number of measured I–V curves, along with the average RMSE, MAE, and solution times are specified.

It is noteworthy to say that the dataset contains curves that correspond to measurements under partial shading and other

TABLE V
AVERAGE RMSE, MAE, AND SOLUTION TIMES (MSEC) OBTAINED WITH THE PROPOSED METHOD WITHOUT REFINEMENT

PV module	# Curves	$\overline{\text{RMSE}}$	$\overline{\text{MAE}}$	$\overline{t_{\text{sol}}}$
aSiMicro03036-Cocoa	39 037	5.93E-04	5.05E-04	8.33
aSiMicro03036-Eugene	43 343	8.21E-04	7.11E-04	8.51
aSiMicro03038-Golden	12 148	7.79E-04	6.63E-04	8.56
aSiTandem72-46-Cocoa	39 186	1.58E-03	1.38E-03	8.09
aSiTandem72-46-Eugene	43 266	1.74E-03	1.53E-03	8.79
aSiTandem90-31-Golden	12 070	2.73E-03	2.38E-03	8.92
aSiTriple28324-Cocoa	38 485	9.59E-03	8.45E-03	9.04
aSiTriple28324-Eugene	42 705	9.46E-03	8.32E-03	9.74
aSiTriple28325-Golden	11 445	1.34E-02	1.17E-02	9.71
CdTe75638-Cocoa	39 080	1.26E-03	1.08E-03	13.07
CdTe75638-Eugene	42 248	1.07E-03	9.11E-04	12.38
CdTe75669-Golden	11 953	1.45E-03	1.22E-03	12.69
CIGS8-001-Cocoa	38 939	1.19E-02	1.04E-02	12.35
CIGS8-001-Eugene	43 146	1.17E-02	1.01E-02	10.15
CIGS1-001-Golden	12 011	8.56E-03	7.49E-03	13.16
CIGS39017-Cocoa	34 775	1.54E-02	1.31E-02	9.92
CIGS39017-Eugene	42 674	1.46E-02	1.25E-02	9.89
CIGS39013-Golden	11 437	1.68E-02	1.44E-02	9.05
HIT05667-Cocoa	38 377	7.18E-03	5.36E-03	13.76
HIT05667-Eugene	43 271	1.00E-02	7.89E-03	14.13
HIT05662-Golden	11 876	5.57E-03	3.76E-03	13.66
mSi0166-Cocoa	36 765	5.21E-03	4.40E-03	12.09
mSi0166-Eugene	43 268	4.27E-03	3.54E-03	10.9
mSi0247-Golden	11 912	5.20E-03	4.40E-03	12.96
mSi0188-Cocoa	39 102	4.92E-03	4.19E-03	10.42
mSi0188-Eugene	43 127	4.03E-03	3.39E-03	11.78
mSi0251-Golden	11 887	4.85E-03	4.15E-03	12.85
mSi460A8-Cocoa	38 929	5.80E-03	4.60E-03	12.62
mSi460A8-Eugene	43 115	4.61E-03	3.73E-03	10.58
mSi460BB-Golden	11 919	1.70E-02	1.44E-02	12.88
xSi12922-Cocoa	38 989	6.08E-03	4.92E-03	12.93
xSi12922-Eugene	43 185	5.98E-03	4.92E-03	12.51
xSi11246-Golden	11 929	5.32E-03	4.47E-03	12.62

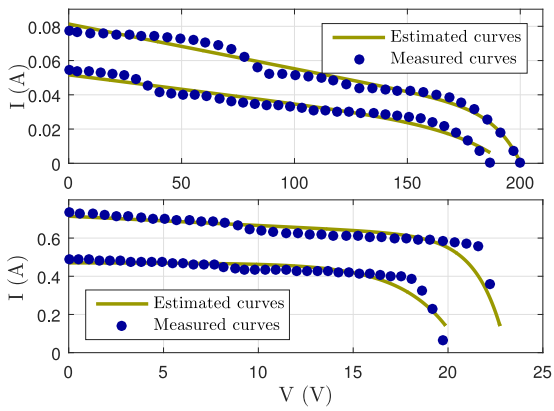

Fig. 5. Parameter identification from I–V curves under partial shading for modules aSiMicro03036–Cocoa (top) and xSi12922–Eugene (bottom).

effects which cannot be captured with the considered single-diode model. The proposed methodology has the potential to automate the identification of these curves as outliers through the evaluation of pertinent error indicators. An example of these curves is depicted in Fig. 5. Once outliers have been identified and removed from the dataset, higher quality solutions may be found featuring lower average RMSE and MAE

TABLE VI
AVERAGE RMSE, MAE, AND SOLUTION TIMES (MSEC) OBTAINED WITH THE PROPOSED METHOD WITH REFINEMENT

PV module	# Curves	$\overline{\text{RMSE}}$	$\overline{\text{MAE}}$	$\overline{t_{sol}}$
aSiMicro03036-Cocoa	39 037	3.00E-04	2.24E-04	19.34
aSiMicro03036-Eugene	43 343	2.50E-04	1.75E-04	35.3
aSiMicro03038-Golden	12 148	2.28E-04	1.88E-04	27.4
aSiTandem72-46-Cocoa	39 186	1.08E-03	9.52E-04	29.38
aSiTandem72-46-Eugene	43 266	9.28E-04	8.15E-04	41.73
aSiTandem90-31-Golden	12 070	1.52E-03	1.32E-03	45.58
aSiTriple28324-Cocoa	38 485	3.71E-03	3.18E-03	50.33
aSiTriple28324-Eugene	42 705	2.99E-03	2.55E-03	66.75
aSiTriple28325-Golden	11 445	3.82E-03	3.19E-03	71.28
CdTe75638-Cocoa	39 080	9.57E-04	7.84E-04	22.25
CdTe75638-Eugene	42 248	9.25E-04	7.59E-04	19.74
CdTe75669-Golden	11 953	1.18E-03	9.59E-04	22.65
CIGS8-001-Cocoa	38 939	5.54E-03	4.30E-03	35.36
CIGS8-001-Eugene	43 146	5.14E-03	4.03E-03	36.36
CIGS1-001-Golden	12 011	3.21E-03	2.55E-03	37.66
CIGS39017-Cocoa	34 775	7.71E-03	6.22E-03	24.25
CIGS39017-Eugene	42 674	7.61E-03	6.18E-03	26.05
CIGS39013-Golden	11 437	9.29E-03	7.64E-03	23.85
HIT05667-Cocoa	38 377	4.84E-03	3.78E-03	32.79
HIT05667-Eugene	43 271	6.46E-03	5.37E-03	40.43
HIT05662-Golden	11 876	3.95E-03	2.20E-03	27.72
mSi0166-Cocoa	36 765	2.93E-03	2.40E-03	34.53
mSi0166-Eugene	43 268	2.69E-03	2.16E-03	31.62
mSi0247-Golden	11 912	3.07E-03	2.56E-03	35.79
mSi0188-Cocoa	39 102	2.38E-03	1.92E-03	29.4
mSi0188-Eugene	43 127	2.21E-03	1.75E-03	32.66
mSi0251-Golden	11 887	2.45E-03	2.01E-03	35.23
mSi460A8-Cocoa	38 929	3.16E-03	2.64E-03	30.42
mSi460A8-Eugene	43 115	2.41E-03	1.97E-03	30.14
mSi460BB-Golden	11 919	8.90E-03	7.55E-03	48.2
xSi12922-Cocoa	38 989	2.75E-03	2.25E-03	33.18
xSi12922-Eugene	43 185	2.48E-03	1.99E-03	34.37
xSi11246-Golden	11 929	2.40E-03	1.78E-03	30.48

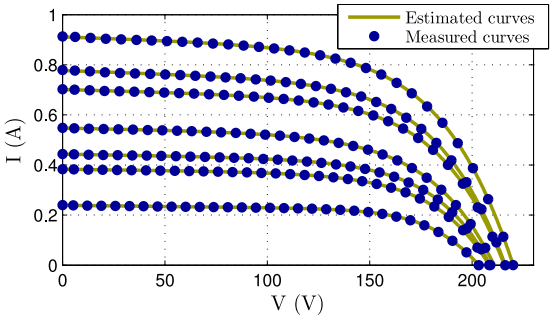

Fig. 6. Measured and estimated I–V curves for PV module aSiMicro03036–Cocoa under a wide range of irradiance conditions and a back surface temperature near to an average value of 35.7°C.

values. For instance, Fig. 6 shows a set of measurements without outliers for the PV module aSiMicro03036–Cocoa. When the proposed parameter extraction methodology is applied to this subset of curves, the resulting average RMSE and MAE were 3.65×10^{-4} and 2.6×10^{-4}, respectively. These values are significantly lower than the average errors obtained considering the whole dataset.

VI. PARAMETER DEPENDENCIES

As demonstrated in the previous section, the low computational complexity and automation capabilities of the proposed methodology enable its application to large sets of experimental curves. This, in turn, makes possible the evaluation of the dependencies of the parameters with respect to the conditions at which the curves were measured. For illustrative purposes, the parameter dependencies of the PV module HIT05662–Golden in the Experiment Set 2 are shown in Fig. 7. While this module belongs to the heterojunction with intrinsic thin-layer technology, analogous figures can be obtained for other PV technologies. The systematic study of these experimental dependencies would enable wide-range operation PV modeling, extending the models proposed in the literature to explain changes in the parameter values with respect to atmospheric conditions [22]–[24].

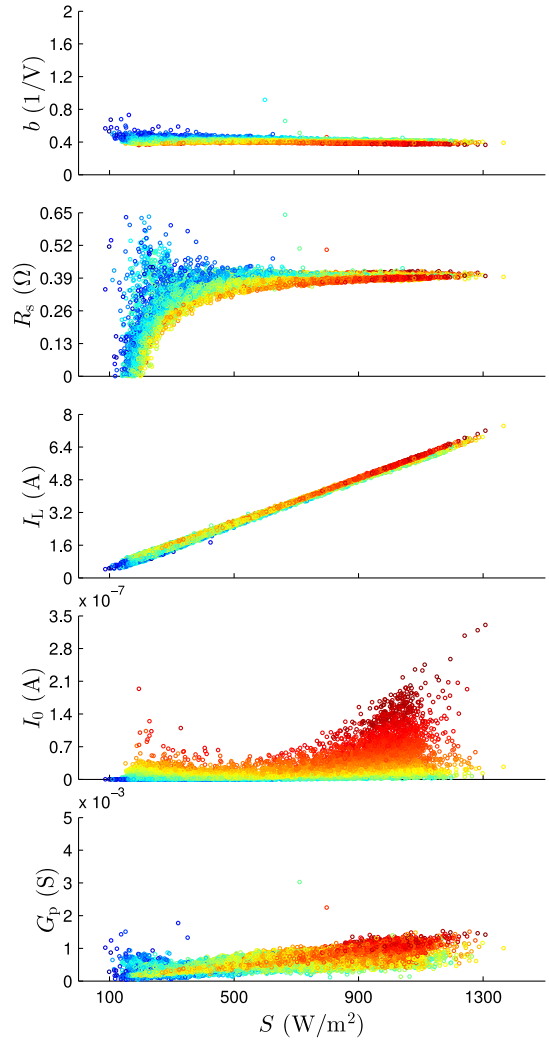

Fig. 7. Dependencies of the parameters b, R_S, I_L, I_0, and G_P for the PV module HIT05662–Golden. The x-axis represents S values, whereas points of the same color correspond to a common T value.

VII. CONCLUSION

An efficient method for the parameter extraction for the single-diode model from experimental I–V curves was developed. An effective dimensionality reduction of the search space is advocated for finding high-quality solutions at a reduced computational cost. Furthermore, the approach does not rely on preliminary data selection, and it can thus be fully automated

without user intervention. The described approach was validated through two sets of experiments. In the first one, two case studies commonly used in the literature were selected in order to perform a comparative evaluation against the best-documented solutions. In the second one, the performance of the proposed methodology was shown through its application to a large-scale repository of I–V curves. The potential of the methodology to study parameter dependencies was also demonstrated. This opens up the possibility to improve the modeling of PV modules. Finally, given its low computational complexity and automation capabilities, the parameter extraction method may be employed in the field for online monitoring, diagnostics, and testing. A computer program implementing this method is available upon request via an e-mail to all interested researchers.

REFERENCES

[1] Navigant Research, Boulder, CO, USA. Distributed solar PV. (2016). [Online]. Available: https://www.navigantresearch.com/research/distributed-solar-pv

[2] J. J. Soon and K. Low, "Optimizing photovoltaic model for different cell technologies using a generalized multidimension diode model," *IEEE Trans. Ind. Electron.*, vol. 62, no. 10, pp. 6371–6380, Oct. 2015.

[3] W. De Soto, S. A. Klein, and W. A. Beckman, "Improvement and validation of a model for photovoltaic array performance," *Solar Energy*, vol. 80, no. 1, pp. 78–88, Jul. 2006.

[4] J. S. Stein, J. Sutterlueti, S. Ransome, C. W. Hansen, and B. H. King, "Outdoor PV performance evaluation of three different models: Single-diode, SAPM and loss factor model," in *Proc. Eur. Photovolt. Solar Energy Conf.*, 2013, pp. 2865–2871.

[5] A. Laudani, F. Riganti-Fulginei, and A. Salvini, "Identification of the one-diode model for photovoltaic modules from datasheet values," *Solar Energy*, vol. 108, pp. 432–446, Oct. 2014.

[6] A. Orioli and A. Di Gangi, "A procedure to calculate the five-parameter model of crystalline silicon photovoltaic modules on the basis of the tabular performance data," *Appl. Energy*, vol. 102, pp. 1160–1177, Feb. 2013.

[7] Y. A. Mahmoud, W. Xiao, and H. H. Zeineldin, "A parameterization approach for enhancing PV model accuracy," *IEEE Trans. Ind. Electron.*, vol. 60, no. 12, pp. 5708–5716, Dec. 2013.

[8] M. Azab, "Identification of one-diode model parameters of PV devices from nameplate information using particle swarm and least square methods," in *Proc. First IEEE Workshop Smart Grid Renewable Energy*, Mar. 2015, pp. 1–6.

[9] K. M. El-Naggar, M. R. AlRashidi, M. F. AlHajri, and A. K. Al-Othman, "Simulated annealing algorithm for photovoltaic parameters identification," *Solar Energy*, vol. 86, no. 1, pp. 266–274, Jan. 2012.

[10] M. F. AlHajri, K. M. El-Naggar, M. R. AlRashidi, and A. K. Al-Othman, "Optimal extraction of solar cell parameters using pattern search," *Renew. Energy*, vol. 44, pp. 238–245, Aug. 2012.

[11] A. Askarzadeh and A. Rezazadeh, "Parameter identification for solar cell models using harmony search-based algorithms," *Solar Energy*, vol. 86, no. 11, pp. 3241–3249, Nov. 2012.

[12] M. S. Ismail, M. Moghavvemi, and T. M. I. Mahlia, "Characterization of PV panel and global optimization of its model parameters using genetic algorithm," *Energy Convers. Manage.*, vol. 73, pp. 10–25, Sep. 2013.

[13] N. Rajasekar, N. K. Kumar, and R. Venugopalan, "Bacterial foraging algorithm based solar PV parameter estimation," *Solar Energy*, vol. 97, pp. 255–265, Nov. 2013.

[14] A. Askarzadeh and A. Rezazadeh, "Artificial bee swarm optimization algorithm for parameters identification of solar cell models," *Appl. Energy*, vol. 102, pp. 943–949, Feb. 2013.

[15] L. L. Jiang, D. L. Maskell, and J. C. Patra, "Parameter estimation of solar cells and modules using an improved adaptive differential evolution algorithm," *Appl. Energy*, vol. 112, pp. 185–193, Dec. 2013.

[16] L. H. I. Lim, Z. Ye, J. Ye, D. Yang, and H. Du, "A linear identification of diode models from single IV characteristics of PV panels," *IEEE Trans. Ind. Electron.*, vol. 62, no. 7, pp. 4181–4193, Jul. 2015.

[17] A. Laudani, F. Riganti-Fulginei, and A. Salvini, "High performing extraction procedure for the one–diode model of a photovoltaic panel from experimental I–V curves by using reduced forms," *Solar Energy*, vol. 103, pp. 316–326, May 2014.

[18] C. W. Hansen, A. Luketa–Hanlin, and J. S. Stein, "Sensitivity of single diode models for photovoltaic modules to method used for parameter estimation," in *Proc. Eur. Photovolt. Solar Energy Conf.*, 2013, pp. 1–7.

[19] W. Marion *et al.*, "User's manual for data for validating models for PV module performance," Nat. Renew. Energy Lab., Golden, CO, USA, Tech. Rep. NREL/TP-5200-61610, Apr. 2014.

[20] H. Tian, F. Mancilla-David, K. Ellis, E. Muljadi, and P. Jenkins, "A cell-to-module-to-array detailed model for photovoltaic panels," *Solar Energy*, vol. 86, no. 9, pp. 2695–2706, Sep. 2012.

[21] G. M. Masters, *Renewable and Efficient Electric Power Systems*. Hoboken, NJ, USA: Wiley, 2013.

[22] A. P. Dobos, "An improved coefficient calculator for the California Energy Commission 6 parameter photovoltaic module model," *J. Solar Energy Eng.*, vol. 134, May 2012, Art. no. 021011.

[23] W. Zhou, H. Yang, and Z. Fang, "A novel model for photovoltaic array performance prediction," *Appl. Energy*, vol. 84, no. 12, pp. 1187–1198, Dec. 2007.

[24] M. Boyd, S. Klein, D. Reindl, and B. Dougherty, "Evaluation and validation of equivalent circuit photovoltaic solar cell performance models," *J. Solar Energy Eng.*, vol. 133, May 2011, Art. no. 021005.

[25] W. R. Esposito and C. A. Floudas, "Global optimization in parameter estimation of nonlinear algebraic models via the error-in-variables approach," *Ind. Eng. Chem. Res.*, vol. 37, no. 5, pp. 1841–1858, May 1998.

[26] A. Jain and A. Kapoor, "Exact analytical solutions of the parameters of real solar cells using Lambert W-function," *Solar Energy Mater. Solar Cells*, vol. 81, no. 2, pp. 269–277, Feb. 2004.

[27] A. Laudani, F. Mancilla-David, F. Riganti-Fulginei, and A. Salvini, "Reduced-form of the photovoltaic five-parameter model for efficient computation of parameters," *Solar Energy*, vol. 97, pp. 122–127, Nov. 2013.

[28] M. J. Bagajewicz and V. Manousiouthakis, "On the generalized Benders decomposition," *Comput. Chem. Eng.*, vol. 15, no. 10, pp. 691–700, Oct. 1991.

[29] G. Cirrincione and M. Cirrincione, *Total Least Squares Problems*. Hoboken, NJ, USA: Wiley, 2010.

[30] Y. Luo and R. Duraiswami, "Efficient parallel nonnegative least squares on multicore architectures," *SIAM J. Sci. Comput.*, vol. 33, no. 5, pp. 2848–2863, Oct. 2011.

[31] R. M. Corless, D. J. Jeffrey, and D. E. Knuth, "A sequence of series for the Lambert W function," in *Proc. Int. Symp. Symbolic Algebr. Comput.*, Jul. 1997, pp. 197–204.

[32] A. Hoorfar and M. Hassani, "Approximation of the Lambert W function and hyperpower function," *Res. Rep. Collect.*, vol. 10, no. 2, pp. 1–5, 2007.

[33] GSL—GNU Scientific Library. (2016). [Online]. Available: http://www.gnu.org/software/gsl/

[34] MPFIT—Robust non-linear least squares curve fitting. (2016). [Online]. Available: http://purl.com/net/mpfit

Alejandro A. Cárdenas (M'06) was born in Osorno, Chile. He received the B.S. and M.S. degrees in electrical engineering from the Universidad Técnica Federico Santa María (UTFSM), Valparaíso, Chile, in 2004 and 2007, respectively, and the Ph.D. degree in operational research from the Universidad de Chile, Santiago, Chile, in 2015.

He is currently a Postdoctoral Fellow in the Department of Electrical Engineering, University of Chile and a Lecturer in the Departments of Electrical and Industrial Engineering, UTFSM. His main research interests include integer programming and large-scale optimization applied to electrical power systems operation and planning.

Miguel Carrasco received the Ingeniería Industrial degree from the Universidad Politécnica de Madrid, Madrid, Spain, in 2006, and the Ph.D. degree from the University of Colorado Denver, Denver, CO, USA, in 2016, both in electrical engineering.

From 2006 to 2010, he was a Research Engineer for the automobile and solar industry in Germany. In 2016, he was with the University of Colorado Denver as a Research Assistant. He was a Visiting Scholar at L'Ecole Supérieure d'Électricité" (Supélec), Gif-sur-Yvette, France, and at the Institut de Recerca en Energia de Catalunya, Barcelona, Spain. He holds a joint patent with the car manufacturer BMW on dynamic modeling of batteries. His research interests include power systems, power electronics and applications to interface renewable sources of energy, distributed generation, and optimization problems.

Fernando Mancilla-David (S'05–M'07) was born in Valparaíso, Chile. He received the B.S. degree in electrical engineering from the Universidad Técnica Federico Santa María, Valparaíso, Chile, in 1999, and the M.S. and Ph.D. degrees in electrical engineering from the University of Wisconsin–Madison, Madison, WI, USA, in 2002 and 2007, respectively.

Since 2007, he has been in the Department of Electrical Engineering, University of Colorado Denver, Denver, CO, USA, where he is an Associate Professor. He is currently a Fulbright Scholar on sabbatical leave at PUC–Rio University, Rio de Janeiro, Brazil. He has been a Visiting Scholar at several research institutions around the world, including ABB Corporate Research, Västerås, Sweden; L'Ecole Supérieure d'Électricité" (Supélec), Paris, France; Technische Universität Berlin, Berlin, Germany; Università degli studi Roma Tre, Rome, Italy; ITMO University, Saint Petersburg, Russia; and the Universidade Federal de Pernambuco, Recife, Brazil. His research interests include power system analysis, energy systems, utility applications of power electronics, control systems, and optimization problems.

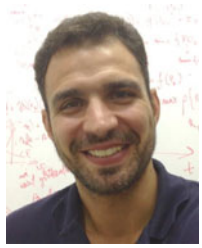

Alexandre Street (S'06–M'10) received the M.Sc. and D.Sc. degrees in electrical engineering (operations research) from the Pontifical Catholic University of Rio de Janeiro (PUC–Rio), Rio de Janeiro, Brazil, in 2004 and 2008, respectively.

From August 2006 to March 2007, he was a Visiting Researcher at the Universidad de Castilla–La Mancha, Ciudad Real, Spain. At the beginning of 2008, he joined PUC–Rio to teach courses on optimization in the Department of Electrical Engineering as an Assistant Professor. He currently holds a tenured position in this department and teaches courses on energy economics, optimization, and statistics. He coordinates the energy research group of the Laboratory of Applied Mathematical Programming and Statistics, and his research interests include: robust and stochastic models for power systems operation and planning, optimization models for optimal investment in renewable energy, optimization methods, and decision making under uncertainty.

Roberto Cárdenas (S'95–M'97–SM'07) was born in Punta Arenas, Chile. He received the B.Sc. degree in electrical engineering from the University of Magallanes, Punta Arenas, in 1989, and the M.Sc. degree in electronic engineering and the Ph.D. degree in electrical and electronic engineering from the University of Nottingham, Nottingham, U.K., in 1991 and 1996, respectively.

From 1989 to 1991 and 1996 to 2008, he was a Lecturer at the University of Magallanes. From 1991 to 1996, he was with the Power Electronics Machines and Control Group, University of Nottingham. From 2009 to 2011, he was with the Department of Electrical Engineering, University of Santiago, Santiago, Chile. He is currently a Professor of power electronics and drives in the Department of Electrical Engineering, University of Chile, Santiago. His main interests are in control of electrical machines, variable-speed drives, and renewable energy systems.

Prof. Cárdenas received the Best Paper Award from the IEEE TRANSACTIONS ON INDUSTRIAL ELECTRONICS in 2005, and he is currently an Associate Editor of this journal.